Fokker-Planck description of single nucleosome repositioning by dimeric chromatin remodelers

Yves Vandecan, Ralf Blossey

Fokker-Planck description of single nucleosome repositioning by dimeric chromatin remodelers

Yves Vandecan and Ralf Blossey
Interdisciplinary Research Institute USR 3078 CNRS and Université de Sciences et de Technologies de Lille, Parc de la Haute Borne, 50 Avenue de Halley, 59658 Villeneuve d'Ascq, France
(Received 18 January 2013; published 30 July 2013)

Recent experiments have demonstrated that the ATP-utilizing chromatin assembly and remodeling factor (ACF) is a dimeric, processive motor complex which can move a nucleosome more efficiently towards longer flanking DNA than towards shorter flanking DNA strands, thereby centering an initially ill-positioned nucleosome on DNA substrates. We give a Fokker-Planck description for the repositioning process driven by transitions between internal chemical states of the remodelers. In the chemical states of ATP hydrolysis during which the repositioning takes place a power stroke is considered. The slope of the effective driving potential is directly related to ATP hydrolysis and leads to the unidirectional motion of the nucleosome-remodeler complex along the DNA strand. The Einstein force relation allows us to deduce the ATP-concentration dependence of the diffusion constant of the nucleosome-remodeler complex. We have employed our model to study the efficiency of positioning of nucleosomes as a function of the ATP sampling rate between the two motors which shows that the synchronization between the motors is crucial for the remodeling mechanism to work.

DOI: 10.1103/PhysRevE.88.012728 PACS number(s): 87.14.gk, 87.15.A−, 87.16.Nn

I. INTRODUCTION

Nucleosome repositioning on DNA substrates can be spontaneous due to thermal fluctuations or forced by adenosine triphosphate–(ATP-) dependent remodelers [1,2]. Recently, *in vitro* experiments and structural analyses have shown the *ATP-utilizing chromatin assembly and remodeling factor* (ACF) to be a dimeric, processive motor which generates center-positioned nucleosomes because it moves the nucleosome more efficiently towards the longer flanking DNA than towards the shorter flanking DNA strands [3,4]. A schematic representation is shown in Fig. 1.

In previous work, we have formulated a stochastic model for this positioning process based on a master equation approach [5]. Although this model predicts reliable velocity profiles and dispersions and furthermore made explicit some details of the fueling mechanism of the ACF motors along with their synchronization, the basic mechanism proposed considers only transitions between discrete intermediate states without any mechanical knowledge of the motor. Despite the fact that discrete intermediates are observed in gel mobility shift experiments, the dynamical frequency resonance energy transfer (FRET) time traces show translocation steps of 7 base pairs (bp), 3 bp, and again 3 bp with finite translocation step times. Here, we propose a continuous repositioning mechanism in terms of a Fokker-Planck equation which, beyond the discrete two-motor model, allows explicit treatment of the thermal diffusion of the nucleosome-remodeler complex. A second aspect is the application of both models to the centering of a nucleosome-remodeler complex as a function of the ATP sampling between the two motors, a situation of relevance for the interpretation of the experimental findings by Narlikar [3,4].

In our Fokker-Planck (FP) model, we retain the explicit description of the two motors as used previously in Ref. [5], but we now require the knowledge of the potentials belonging to the chemical states. The FP model allows for a detailed chemomechanical description of the motors, although no experimental effective driving potential [6] of ACF has been derived so far in the literature. We assume that in the chemical states of ATP hydrolysis (the activated ADP*Pi states in Ref. [3]) basic effective driving potentials are acting which, as will be seen later on, are capable of centering the nucleosome with respect to the DNA substrate. These effective driving potentials are purely power stroke potentials in which the chemical energy of ATP hydrolysis is converted into mechanical work done along a motor step [7]. Experimentally, the ability of chromatin remodelers to translocate nucleosomes under high forces points to a motor with a power stroke mechanism rather than a Brownian ratchet mechanism rectifying (large) thermal fluctuations [6,8,9], which motivates our choice.

The origin of power strokes is related to the tightening of the remodeler with DNA, pulling the DNA flanking length into the nucleosome [8,10] and "tracking" of the nucleosome-remodeler complex with respect to the DNA. This means that the motor translocates along the DNA, and ATP is required for the unidirectional diffusion of the bulge towards the distal end of the nucleosome. The energy release of ATP hydrolysis, required for a translocation of size $\Delta\ell$, corresponds to a potential energy decrease ΔU_d. The parameter ℓ determines the position of the nucleosome with respect to the DNA strand. Based on experimental findings, one ATP molecule is consumed, releasing $12k_BT$ during ATP hydrolysis [11], for a 13 bp translocation [12]. The slope of the power stroke potential $\Delta U_d/\Delta\ell$ equals a generated force $F \approx k_BT/\text{bp}$.

The other remaining chemical states, with a reduced remodeler-DNA interaction [10], are mainly governed by the thermal motion of DNA. These thermal fluctuations are incorporated in the thermal diffusion constant of the nucleosome-remodeler complex, D_{NR}, which can be due to twist or loop diffusion. Experimental thermal diffusion constants of the nucleosome without the presence of the (ACF) remodeler D are in the order of 1 bp^2/s. The diffusion of 10 bp loops results in the rather low theoretical value of $D = 0.1\ \text{bp}^2/\text{s}$ while twist diffusion, in combination with a positioning sequence, predicts a higher value of $D = 7\ \text{bp}^2/\text{s}$ [2,13].

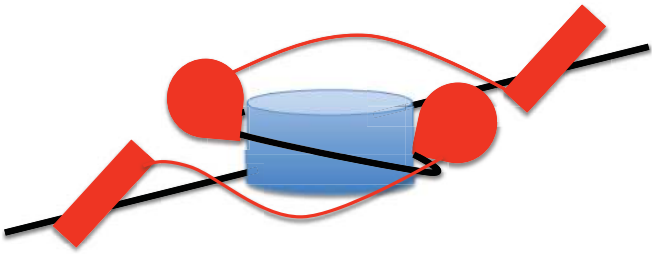

FIG. 1. (Color online) Schematic representation of the geometry of the ACF-nucleosome complex. The nucleosome is shown as a cylinder, on which two remodelers are placed with their central motor unit, while the directional domain (SANT-SLIDE), presented as a rectangle, attaches to the linker DNA. The displacement of the complex is controlled by the synchronization of the two remodelers.

Using the theoretical Einstein force scale [11], we estimate the thermal diffusion constant of the nucleosome-remodeler (NR) complex to be $D_{NR} = (k_B T/F)V$, via the experimental local translocation speed V in the frequency resonance energy transfer time traces. We quantify V by (13 bp)k_{tr}, with $1/k_{tr}$ as the effective translocation time required to translocate 13 bp along the DNA strand [5]. Although the Einstein force scale is strictly only valid for Brownian particle motion in thermal equilibrium, its application to an activated molecular motor ACF still yields acceptable results [11]. These computations reveal an ATP dependence of the diffusion constant of the nucleosome-remodeler complex, with a higher mobility at higher ATP concentrations. The latter refers to ATP-dependent looping and possibly reflects a remodeler-mediated looping mechanism depending on the concentration of ATP, as experimentally suggested [14,15].

Our paper is organized as follows: We derive a system of five coupled Fokker-Planck equations which represent the time evolution of the probability functions to be in the corresponding five chemical states. Next, a comparative study of this continuum model with the discrete motor models is presented, in which we discuss the similarities, (dis)advantages, and insights of our Fokker-Planck model. We close with a detailed discussion of the ATP dependence of the diffusion constant.

II. A FOKKER-PLANCK MODEL OF ACF REPOSITIONING

In considering a highly processive motor we restrict our analysis to the actual repositioning process without dissociation of the nucleosome-remodeler complex. Five chemical states are considered to describe the repositioning process by dimeric ACF. We catalog the states of the two motors by a two-valued variable in which each value represents the state of an individual motor. The first chemical state is an apo state (0,0) without ATP binding. The next two chemical states are (ATP,0) and (0,ATP) with ATP bound to the left (right) ATPase unit bound at nucleosomal superhelical locations $(-2,2)$, respectively. The remaining two states correspond to ATP in activated form, i.e., (ADP*Pi,0) and (0,ADP*Pi) in which the left (right) motor translocates the complex along the DNA strand, decreasing the ATP energy. The transition scheme of these chemical states is shown in Fig. 2.

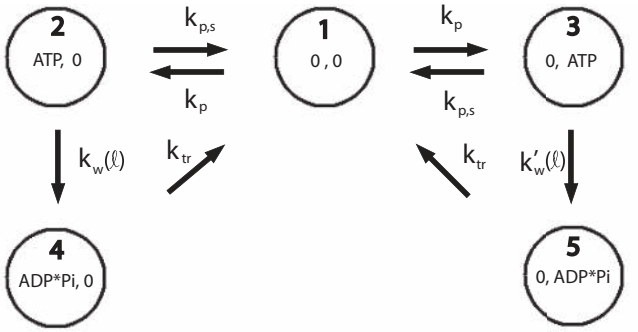

FIG. 2. The two-motor model with a power stroke is schematically depicted with transitions between the five chemical states. The chemical states (0,0), (ATP,0), (0,ATP), (ADP*Pi,0), and (0,ADP*Pi) are numbered from 1 to 5, respectively. The rate $k_w(\ell)$ [or $k'_w(\ell)$] is the length-dependent transition rate from the (ATP,0) [or (0,ATP)] state to the active translocation state (ADP*Pi,0) [or (0,ADP*Pi)]. The rate k_{tr}, assumed to be length independent, is the transition rate from the active translocation state [(ADP*Pi,0) or (0,ADP*Pi)] to the apo state (0,0). The rate k_p is the ATP binding rate from the (0,0) to the (ATP,0) [or (0,ATP)] state. Finally, the rate $k_{p,s}$ is the transition rate which makes ATP sampling possible; it is the ATP unbinding rate of the left (or right) motor to the apo state, with the possibility of subsequent binding to the right (or left) motor.

The transition rate k_p is for the transition from the apo state to (ATP,0) or (0,ATP). The rate $k_{p,s}$ corresponds to the unbinding of ATP from (ATP,0) or (0,ATP) without being hydrolyzed. The former rate is related to ATP-loading steps while the latter introduce the sampling step between the motors in which a nonhydrolyzed ATP is unbound from the "left" motor and can be bound to the "right" motor or vice versa, which is why we also call this rate the "sampling rate." The rates $k_w(\ell)$ and $k'_w(\ell)$ correspond to the ATP "activation" time to initiate ATP hydrolysis, allosterically dependent on the DNA linker length ℓ [16]. From these FRET experiments of nucleosomes with different flanking lengths, a plot of the natural logarithm of the rate constant $\ln(k)$, proportional to the activation energy of the reaction, versus their DNA flanking length is a straight line. In our model, we assume for the activation time an exponential dependence on the linker length ℓ, i.e.,

$$k_w(\ell) = \alpha e^{a(80-\ell)}, \tag{1}$$

$$k'_w(\ell) = \alpha e^{a\ell}, \tag{2}$$

where $a = 0.077$ bp^{-1} [5] is the intrinsic linker length dependence, α a proportionality constant, and the linker length ℓ varies between 0 and 80 bp. The end-positioned nucleosomes $0N80$ and $80N0$ correspond to $\ell = 0,80$ bp. Between these extreme values of ℓ, all other DNA linker lengths are possible. In the case of the end-positioned nucleosome $0N80$ ($\ell = 0$), the activation time rate $k_w(\ell)$ of the (ATP,0) to (ADP*Pi,0) state differs by an exponential factor from the rate $k'_w(\ell)$ of the (0,ATP) to the (0,ADP*Pi) state [5]. Concerning the motion of the remodeler-nucleosome complex, suppose we have an end-positioned nucleosome $\ell = 0$: Starting from the apo state, ATP can bind to the left or to the right motor, i.e., the (ATP,0) or (0,ATP) state. In the (ATP,0) the activation rate $k_w(\ell = 0)$ has a high value so that the nucleosome-remodeler complex

probably enters (ADP*Pi,0) before dissociating to the apo state, while in the (0,ATP) state $k'_w(\ell = 0)$ is practically zero, and therefore ATP will with high probability to dissociate before entering the (0,ADP*Pi) state. As a consequence, the nucleosome-remodeler complex is pushed towards larger ℓ. Finally, the rate k_{tr} is the inverse of the period during which the active translocation takes place due to ATP hydrolysis. We remark that the total rates k (k') from [(ATP,0) (0,ATP)] to the apo state (0,0) equal

$$k = \frac{\alpha\, e^{a(80-\ell)}}{1 + \frac{\alpha}{k_{tr}} e^{a(80-\ell)}}, \tag{3}$$

$$k' = \frac{\alpha\, e^{a\ell}}{1 + \frac{\alpha}{k_{tr}} e^{a\ell}}. \tag{4}$$

For $\frac{\alpha}{k_{tr}} \ll 1$ and small values of ℓ, Eq. (4) reduces to the experimental transition rates of the form $k_0 e^{a\ell}$, $20 \leqslant \ell \leqslant 60$ bp, between the intermediates in the previous one- and two-motor models [5]. The factor α can thus be approximated by the value of k_0 in previous work. Importantly, the equation for k' has the proper shape to saturate at higher values of ℓ, resembling the cutoff at 60 bp discussed in the previous model. A similar reasoning can be used for k. The exponential dependence of only the activation time on the DNA linker length, and not the translocation time ($1/k_{tr}$) itself (to less extent), consequently has experimental justification. Hydroxyl radical footprint studies show that, after ATP binding, the remodeler interaction with the DNA flanking length increases its protection pattern (i.e., the covering of the DNA substrate), allosterically triggering ATP hydrolysis [10,16].

Once the transitions between the chemical states are defined, the dynamics can be translated into five coupled Fokker-Planck equations that allow computation of the probability distributions $P_\sigma(\ell,t)$ of the five chemical states, $\sigma = 1,\ldots,5$ (see Fig. 2), as a function of the ℓ state and time t. The five coupled partial differential equations for $P_\sigma(\ell,t)$ can be written as

$$\partial_t P_\sigma(\ell,t) + \partial_\ell J_\sigma(\ell,t) = \sum_{\sigma'=1}^{5} M_{\sigma\sigma'} P_{\sigma'}(\ell,t), \tag{5}$$

with the probability flux

$$J_\sigma(\ell,t) = -\frac{1}{\gamma}\partial_\ell U_\sigma(\ell) P_\sigma(\ell,t) - D_{NR}\partial_\ell P_\sigma(\ell,t). \tag{6}$$

Here $U_\sigma(\ell)$ is the potential (as a function of ℓ) in the chemical state σ; see Fig. 3. Further, D_{NR} denotes the thermal diffusion constant of the nucleosome-remodeler complex, the friction coefficient $\gamma = k_B T/D_{NR}$, and $M_{\sigma\sigma'}$ the matrix elements of

$$\mathbf{M} = \begin{pmatrix} -2k_p & k_{p,s} & k_{p,s} & k_{tr} & k_{tr} \\ k_p & -k_w(\ell) - k_{p,s} & 0 & 0 & 0 \\ k_p & 0 & -k'_w(\ell) - k_{p,s} & 0 & 0 \\ 0 & k_w(\ell) & 0 & -k_{tr} & 0 \\ 0 & 0 & k'_w(\ell) & 0 & -k_{tr} \end{pmatrix}.$$

The presumed expressions for the potentials $U_4(\ell)$ and $U_5(\ell)$ in the activated states (ADP*Pi,0) and (0,ADP*Pi) are $\mp(k_B T/\text{bp})\ell$, respectively, and thus proportional to the linker length ℓ. The decreasing (or increasing) straight lines are pure power stroke potentials, tracking the complex in a definite direction of ℓ with the ATP energy consumption along the straight line. The slopes of the power stroke potentials $U_4(\ell)$ and $U_5(\ell)$ are $\mp k_B T/\text{bp}$. The latter expressions are based on the experimental fact that a motor step size of 13 bp corresponds to an energy decrease of $12 k_B T$, the energy release due to ATP hydrolysis of one ATP molecule [11,12]. The remaining potentials for $\sigma' = 1,2,3$ vanish identically. In the discussion of the mathematical technique to solve the equations, given below, the zero-flux boundary conditions are replaced by an extension of the ℓ states and the introduction of an artificial confinement potential. We further introduce the total probability distribution

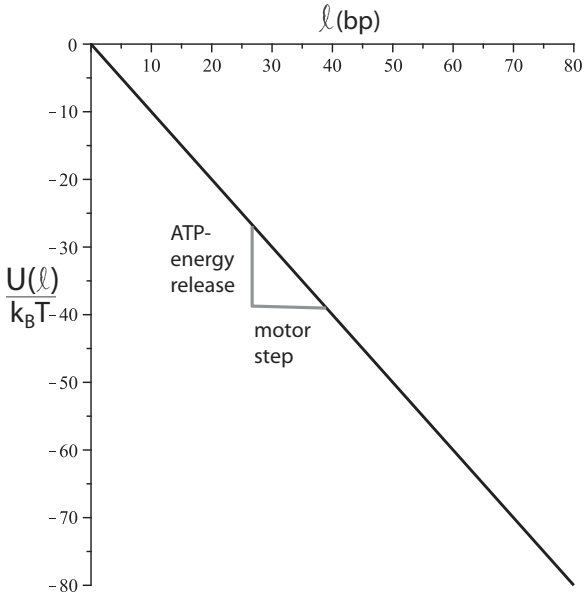

FIG. 3. The potential $U(\ell)$ in the Fokker-Planck equation.

$$P_t(\ell,t) = \sum_{\sigma=1}^{5} P_\sigma(\ell,t). \tag{7}$$

It is interesting to note that, from the Fokker-Planck equations which describe a continuous stochastic process, we are able to go back to an equivalent master equation, describing a jump process [17]. In our case, this can be achieved by allowing only transitions between the chemical states at definite $\ell = \ell_i$ states. For example, if transitions at each base pair are considered, then we end up with an equivalent master equation modeling transitions among 160×5 states.

We expect the remodeler to be incapable of translocating with too short DNA linker lengths, so that for these ℓ states the power stroke potentials $U_4(\ell)$ and $U_5(\ell)$ should be flat. However, the states with too short linker lengths will not be reached due to the inability for ATP hydrolysis. In order to simplify the calculations, we may assume $U_4(\ell)$ and $U_5(\ell)$ equal to $\mp(k_B T/\text{bp})\ell$ for all ℓ states without much affecting the numerical outcome.

Concerning the translocation step time and the kinetic pauses from the FRET time traces [14], we presume an effective 13 bp translocation step time (sum of the experimental 7 bp, 3 bp, and 3 bp translocation step times) and an effective pause (sum of the experimental first, second, and third kinetic pauses), as in Ref. [5]. The thermal diffusion constant of the nucleosome-remodeler complex, D_{NR}, equals $(k_B T/F)V$

TABLE I. Estimated values of the model parameters as functions of the ATP concentration [5,14].

[ATP] (μM)	$\alpha = k_0$ (min^{-1})	k_{tr} (s^{-1})	k_p (s^{-1})	D_{NR} (bp^2/s)
2	0.02	0.03	0.03	0.4
20	0.3	0.5	0.3	6.5
200	0.5	0.8	0.6	11
2000	0.6	1	0.9	13

using the Einstein force scale. The generated force $F = \Delta U_d/\Delta\ell$ is theoretically determined by the energy release ΔU_d of one molecule of ATP during a translocation $\Delta\ell = 13$ bp. The local translocation speed $V = (13\text{ bp})k_{tr}$ is obtained via the experimentally established effective translocation time $1/k_{tr}$. If we again set the sampling rate $k_{p,s}$ equal to k_p, then the ATP loading rates k_p (and $k_{p,s}$) in this Fokker-Planck model are found from

$$t_k = \frac{2}{k_p} + \frac{1}{k_w(0)}, \tag{8}$$

with t_k as the effective kinetic pause. $k_w(0)$ is the activation time rate [see formula (1)] of the end-positioned nucleosome needed to address the experimental FRET time traces. A summary of the computed model parameters for different values of ATP is given in Table I.

In order to numerically solve the coupled Fokker-Planck equations, we employ a simple finite difference method. At time t_i and spatial position ℓ_p, the derivative $\partial_\ell P_\sigma(\ell_p,t_i)$ and the second derivative $\partial_\ell^2 P_\sigma(\ell_p,t_i)$ are numerically computed by the centered-difference approximation,

$$\partial_\ell P_\sigma(\ell_p,t_i) = \frac{P_\sigma(\ell_p+\Delta\ell,t_i) - P_\sigma(\ell_p-\Delta\ell,t_i)}{2\Delta\ell} + O(\Delta\ell^2), \tag{9}$$

$$\partial_\ell^2 P_\sigma(\ell_p,t_i) = \frac{P_\sigma(\ell_p+\Delta\ell,t_i) - 2P_\sigma(\ell_p,t_i) + P_\sigma(\ell_p-\Delta\ell,t_i)}{\Delta\ell^2} + O(\Delta\ell^2). \tag{10}$$

Next we can compute the corresponding increment $\Delta P_\sigma(\ell_p,t_i)$ by $\partial_t P_\sigma(\ell_p,t_i)\Delta t$ and applying Eq. (5). Instead of imposing more complicated zero-flux boundary conditions, we extend the interval for ℓ from [0, 80] to $[0-\delta_I, 80+\delta_I]$, and put the system in a confinement potential (see the Appendix), preventing a probability flux at the boundaries. The boundary condition $P(0-\delta_I,t) = P(80+\delta_I,t) = 0$ for all t then conceptually suffices to conserve total probability within the confinement potential. In the numerical computations δ_I is set to 40 bp. As a measure for the numerical accuracy, we check the conservation of the total probability as a function of the time. A spatial step $\Delta x = 0.5$ bp and time steps $\Delta t = 0.02$ and 0.001 s for 2, 20 200, and 2000 μM ATP, respectively, produce an approximate numerical solution that leaves the total probability unaltered within a 0.2% "band" around probability 1 among the ℓ states. An increase in accuracy narrows this band, but also significantly enlarges the numerical computation time. (A general disadvantage of the FP model is that it can only be solved numerically and not exactly, as could be done with the master equation model.) As can be easily checked numerically, stationary probability distributions are rather insensitive to distinct step sizes. Stationary probability distributions, because they are generally independent of the initial distribution, have the advantage to find first a rough approximate expression with less accurate step sizes, after which a numerically accurate stationary distribution is obtained with refined step sizes.

III. RESULTS AND DISCUSSION

A. Velocity profiles

For our Fokker-Planck model we use the finite difference approximation scheme described above to compute the probability density functions $P_t(\ell,t)$ for the four concentrations of ATP given in Table I. As initial distribution for the probability distribution we choose

$$P_t(\ell,t=0) = \frac{1}{2\pi\sigma^2}\exp\left(-\frac{(\ell-10)^2}{2\sigma^2}\right), \tag{11}$$

reflecting a family of nucleosomes (nearly end positioned) around a mean $\ell = 10$ bp, with a standard deviation $\sigma = 1$ bp. The average velocity profiles $\langle v\rangle$ (see Fig. 4) are obtained by numerical integration of the expression

$$\langle v\rangle = \frac{d}{dt}\int_{\ell_i}^{\ell_f} d\ell\, P_t(\ell,t)\ell, \tag{12}$$

with ℓ_i and ℓ_f the values of the initial and the final ℓ states, respectively. The velocity profiles from the continuum model [see Fig. 4(a)] are similar to our two previous motor models (single motor and two motors) with transitions between the seven intermediates [5]. A family of end-positioned nucleosomes around the mean $\ell = 0$, but allowing for negative ℓ states, returns velocity profiles that overall coincide better with the previous discrete two-motor model, as they should [see Fig. 4(b)]. This accordance justifies the assumptions of the underlying physics in the Fokker-Planck model, opening a more detailed level of the physical description of the remodeling mechanism by the ACF: (1) The energy release per ATP molecule contributes to an average translocation of 13 bp; (2) the separate implementation of the ATP consumption required for centering or localizing the nucleosome with respect to DNA, and of the thermal fluctuations via the thermal diffusion constant; (3) the ATP concentration dependence of the diffusion constant of the nucleosome-remodeler complex D_{NR}; and (4) the argument that the activation time (to enter the ADP*Pi state) is exponentially dependent on the linker length ℓ and not (or to less extent) the lifetime of the ADP*Pi state itself—but certainly on this point more experimental evidence is called for. So far, there exists no experimental evidence as to which step of the ATPase cycle the DNA flanking length participates in Ref. [4].

B. Sampling between the motors

In our previous paper [5], we showed that a proper sampling rate is required for center positioning of the nucleosome with respect to the DNA strand. Here we go one step further. In order to quantify the importance of sampling, or when the desynchronization becomes appreciable, we examine the

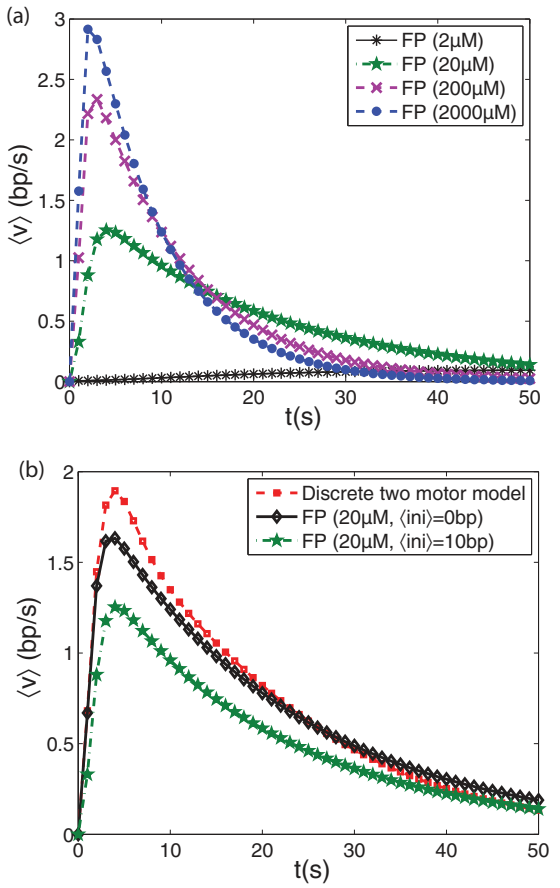

FIG. 4. (Color online) (a) The velocity profiles of the continuum Fokker-Planck model for different concentrations of ATP, starting from a Gaussian initial distribution with an initial mean of 10 bp and standard deviation $\sigma = 1$ bp. (b) A comparison of the velocity profiles of the discrete two-motor model and the Fokker-Planck model, for two distinct initial distributions with an initial mean of 0, 10 bp and standard deviation $\sigma = 1$ bp.

effect of tuning down the sampling rate on the stationary probability distribution. All other parameters retain the same values as in the proper sampling case. The time to reach the stationary probability distribution from an end-positioned nucleosome rapidly increases when tuning down the sampling rate. According to the continuum model, a lowering of the sampling rate becomes appreciable at ≈0.1–0.05 times the initial value (see Fig. 5), similarly to the discrete two-motor model (see below). A decrease of the sampling rate by a factor of 100 generates a bimodal stationary probability distribution with a clear dip at $\ell = 40$ bp; see Figs. 5 and 6. We obtain a bimodal distribution when the sampling rate is highly reduced, but it is broadened by thermal fluctuations.

We compare our findings for the Fokker-Planck model with those from the discrete two-motor model (concerning the mathematical framework of the latter we refer to [5]). The numerical solution of the Fokker-Planck model has the disadvantage of requiring large computation times while the matrix of the discrete two-motor model is quickly diagonalized with standard computational software packages such as MAPLE. As can be seen from Fig. 7, the influence of the decreased sampling rate is noticeable at ≈0.1–0.05 times the initial value, as for

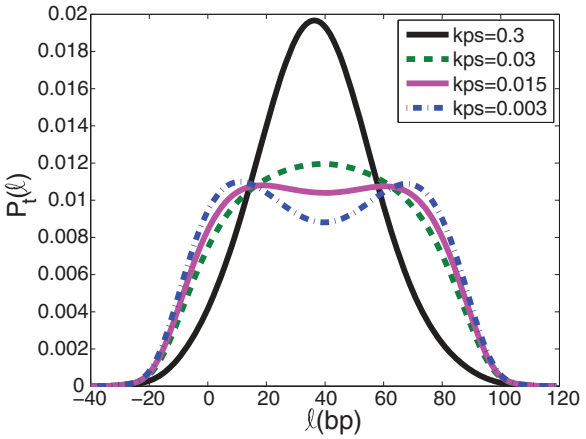

FIG. 5. (Color online) Near steady-state probabilities of the continuum Fokker-Planck model as a function of a reduced sampling rate $k_{p,s}$ (with an ATP concentration of 20 μM). The time t equals 50, 300, 400, and 500 s for the diminished sampling rates $k_{p,s} = 0.3$, 0.03, 0.015, and 0.003 (in units of s^{-1}), in that order. At a reduction of ≈0.05 times the initial value, the highest steady-state probability does not belong to the center-positioned ℓ state anymore. The distribution turns from a monomodal to a bimodal behavior.

the continuum model. Below the critical sampling rate (≈0.05 times the initial value), the center-positioned state has not the highest probability anymore in steady state. Decreasing the

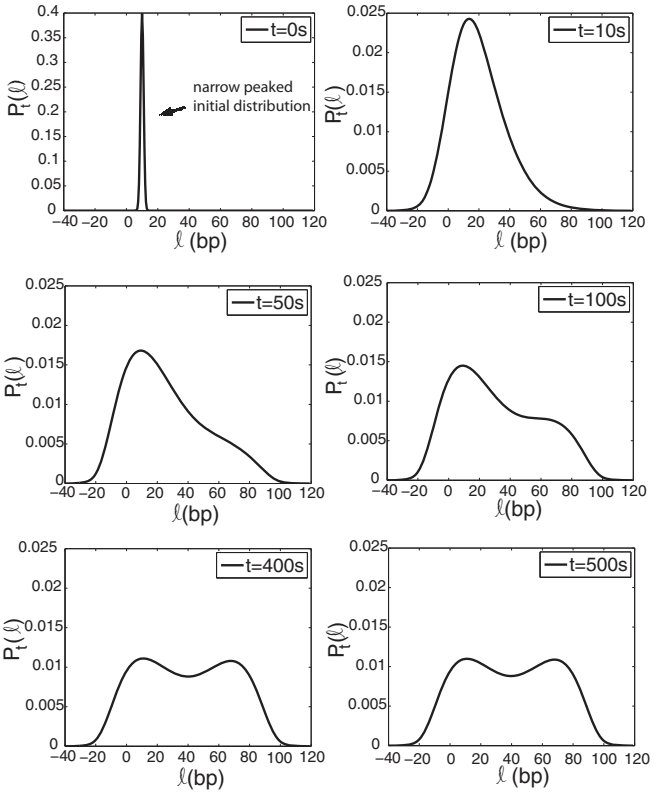

FIG. 6. The transient probability flow from a family of initially end-positioned nucleosomes (around the mean $\ell = 10$ bp and standard deviation $\sigma = 1$ bp) to the other ℓ states is depicted in the case of a sampling rate reduced by a factor of 100. The ATP concentration equals again 20 μM.

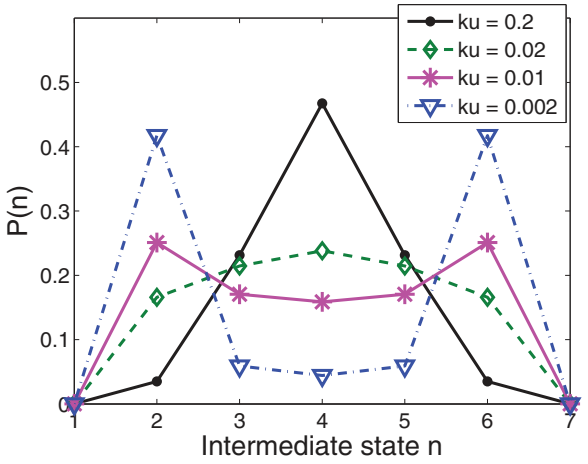

FIG. 7. (Color online) The steady-state probability distribution of the two-motor model as a function of a reduced sampling rate k_u. At a reduction of ≈0.05 times the initial value, the highest steady-state probability does not belong to the center-positioned intermediate anymore. The distribution turns from a monomodal to a bimodal behavior. The considered system has an ATP concentration of 20 μM with a rough approximation for k_c and k_I and high processivity (see [5]).

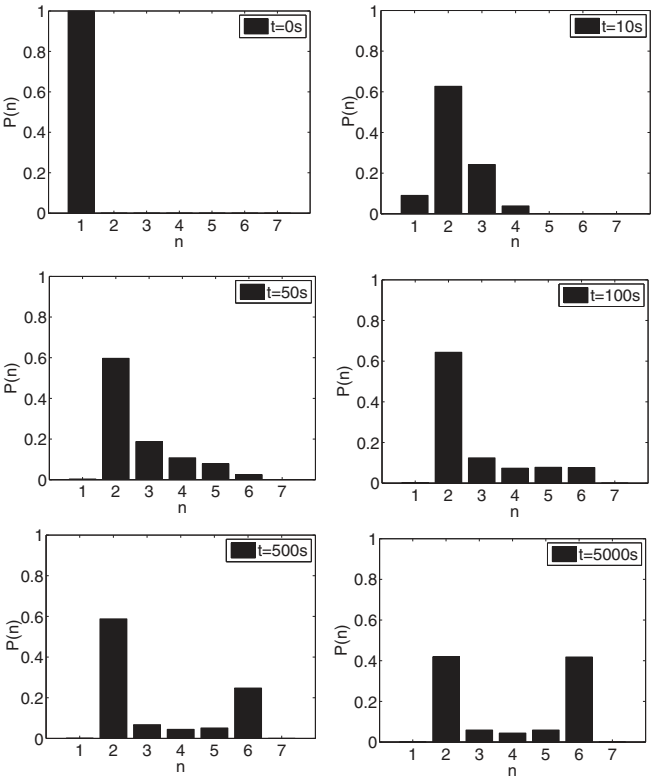

FIG. 8. For the discrete two-motor model, the transient probability flow from an initially end-positioned nucleosome to the other intermediates is depicted in the case of a sampling rate reduced by a factor of 100 (with an ATP concentration of 20 μM). Initially, the probability flows into the $n = 1$ state, followed by a slow probability flow into the mirror state $n = 6$, through the intermediates $n = 2, 3, 4, 5$. Finally, the nucleosome is not center positioned anymore with highest probability in the steady state.

sampling rate 100 times or more generates a bimodal stationary probability distribution with two peaks at intermediate $n = 1$ and the mirror state intermediate $n = 6$ [5]. The resulting behavior is independent of the ATP concentration.

It is interesting to investigate the transient probability flow, and thus how these states appear. For that reason, we show the probability distributions at the times 0, 10, 50, 100, 500, and 5000 s. From Fig. 8, we clearly see that, a short time after the remodeling initiation (10 s), there is a considerable probability flow from $n = 0$ to $n = 1$. Next, the probability at $n = 0$ is completely gone and at larger times, there is a slow probability flow from $n = 1$ towards the mirror state $n = 6$ through the intermediates $n = 2,3,4,5$. In the limit of vanishing sampling rate, we note two absorption points in the scheme of the two-motor model, i.e., the (0,ATP) motor state in $n = 1$ and the (ATP,0) motor state in $n = 6$. A sufficient sampling rate is required to overcome these absorption points and induces a moderately absorbing intermediate $n = 4$, the center-positioned nucleosome. The continuum Fokker-Planck model does not have these absorbing ℓ states due to thermal fluctuations.

In gel mobility shift experiments [12], in contrast with the ACF, the catalytic subunit SNF2h alone produces intermediates with nearly equal probability and remodels more slowly. Still, one may expect SNF2h to act as a dimer [3,5] in the apo state. According to our current models in this paper, this observation indicates a reduced sampling rate (in the vicinity of the critical sampling rate) which predicts intermediates with equal probability. The noncatalytic subunits Acf1 of the ACF remodelers seem therefore to be responsible for an optimal synchronization between the two catalytic subunits SNF2h. The synergistic interaction of the noncatalytic subunit Acf1 and the catalytic subunit to reposition nucleosomes is already mentioned in Refs. [18,19]. Moreover, the experimentally longer repositioning time of SNF2h relative to ACF [18] is in accordance with a lower sampling rate in our models, too.

C. The diffusion constant of the nucleosome-remodeler complex

The ATP-concentration dependence of the diffusion constant of the nucleosome-remodeler complex, D_{NR}, deserves some special attention. Theoretical calculations show a thermal repositioning of nucleosomes through the creation of loops with a thermal diffusion constant $D = 0.1$ bp^2/s [2,13]. Experiments confirm these values [20]. From the FRET time traces we extract that D_{NR} is higher than 0.1 bp^2/s, and strongly increasing with ATP concentration. This originates probably from the partial loosening of attachment of the DNA around the nucleosome, after the consumption of one ATP molecule in the activation step [4,5]. More specifically, a diminished histone-DNA interaction results in an augmented thermal diffusion constant, as can be derived from the combination of the theoretical expression of the thermal diffusion constant D of a single nucleosome [13,21],

$$D = \frac{k_B T}{\eta L_o}\left(\frac{\Delta L}{L^*}\right)^2 e^{-\Delta U/k_B T}, \tag{13}$$

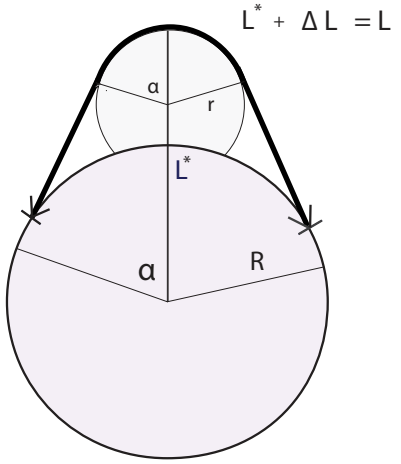

FIG. 9. (Color online) The circle-line approximation, following Ref. [22]. Loop opening angle α, excess loop length L, exposed loop length L^*, nucleosomal radius R, and loop curvature $\kappa = 1/r$.

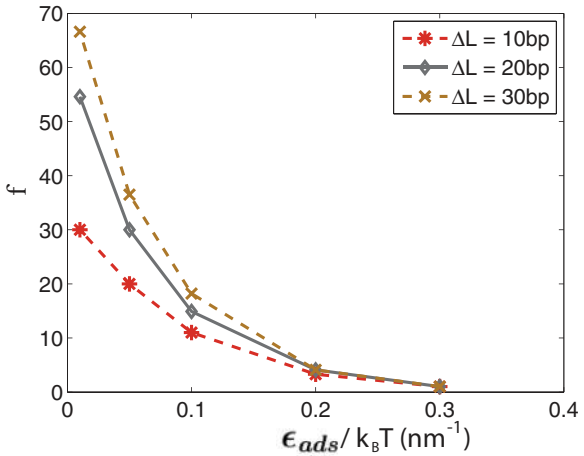

FIG. 10. (Color online) The factor f, Eq. (15), with optimal opening angle α for several histone-DNA adsorption energies ϵ_{ads}.

and the circle-line approximation for simple DNA loops [22] (see Fig. 9),

$$\Delta U = 2\alpha\left(A\frac{\tan(\alpha)-\alpha}{2R[\tan(\alpha)-\alpha]-\Delta L}+R\epsilon_{\text{ads}}\right). \quad (14)$$

In Eq. (13) the symbols L_o, L^*, ΔL, ΔU, η, and k_BT denote the wrapped length of DNA around the nucleosome, the loop's exposed length on the nucleosome, the excess length of the loop, the excess energy of the loop, the viscosity, and the thermal energy, respectively. In Eq. (14) the symbols α, A, R, and ϵ_{ads} are the loop's opening angle, the bending rigidity, the nucleosomal radius, and the net adsorption energy per unit length of the histone-DNA contacts. The loosened state corresponds to a decrease in net adsorption energy ϵ_{ads}. Keeping all the parameters fixed except for the opening angle α, ΔU can be minimized over the opening angles α. We then obtain the minimal loop energy $\Delta U = \Delta U_{\text{min}}$ for an opening angle α_{min}.

It is reasonable for a start to assume that D_{NR} has the same mathematical form as Eq. (13), the thermal diffusion constant D of a single nucleosome. According to Eq. (14), a reduction of $\epsilon_{\text{ads}} \approx 0.3k_BT$/nm to, let us say 0.1 k_BT/nm, lowers the minimal loop energy ΔU_{min} by $\approx$(2–3)k_BT for a fixed $\Delta L = 10$ bp. The corresponding opening angle α_{min} remains practically the same. We consider only small loops for thermal repositioning in the presence of the remodeler ACF. Large loops, although energetically more favorable, should lead to superdiffusive behavior that has not been observed experimentally [22]. As a consequence, the thermal diffusion constant of the nucleosome-remodeler complex, D_{NR}, is multiplied by a factor $\approx$20, and we acquire elevated values of the thermal diffusion constant D_{NR}. In Fig. 10 we show the factor

$$f = e^{[\Delta U_{\text{min}}(\epsilon_{\text{ads}}=0.3)-\Delta U_{\text{min}}(\epsilon_{\text{ads}})]/k_BT} \quad (15)$$

for small loops (with optimal opening angle α) as a function of ϵ_{ads}. One might speculate that ATP is required to hold the nucleosome [4,5] permanently in this loosened state with a lower net adsorption energy. At a low ATP concentration of 2 nM, a reduced ATP supply manages consequently only a slight decrease in net adsorption energy with a $D_{NR} \approx 0.4$ bp^2/s in the vicinity of the thermal $D_{NR} \approx 0.1$ bp^2/s without ATP consumption. High concentrations of ATP allow the formation of a highly loosened state with the thermal diffusion constant $D_{NR} = 1$–10 bp^2/s. To conclude, in the case of thermal repositioning without the presence of the ACF remodeler, the thermal diffusion constant is approximately 0.1 bp^2/s. In the presence of the ACF remodeler and ATP, our estimations point to an elevated thermal diffusion constant D_{NR} due to the loosening of the histone-DNA contacts after the activation step.

IV. CONCLUSION

In this paper we formulated and solved a system of five coupled Fokker-Planck equations with transitions between five chemical states, thereby modeling the repositioning mechanism by ACF. The computed velocity profiles from the probability distributions are similar to the profiles of discrete motor models, and thus in accordance with experiments. This establishes the experimental validity of the continuum model for properly chosen parameter values and allows us to gain insight into a lower-level, chemomechanical description of the ACF remodeler, beyond considering only transitions between discrete intermediates in steps of 13 bp [5].

To start with, dynamical FRET studies of ACF show a gradual decrease in FRET intensity, reflecting a continuous repositioning process. Next, the slope of the pure power stroke is directly linked with the energy release during ATP hydrolysis, i.e., an energy of $\approx 12k_BT$ per ATP molecule for a translocation of 13 bp. We stress, as the third important aspect of the Fokker-Planck description, the ability to incorporate thermal fluctuations, which is lacking in the discrete two-motor model. In our Fokker-Planck description, we separately implement the thermal fluctuations using the thermal diffusion constant of the nucleosome-remodeler complex, D_{NR}, and the ATP-dependent translocation mechanism of the remodeler along the DNA strand using the power stroke potentials. The

thermal diffusion constant tends to broaden the probability distributions over the set of nucleosomal positions while the ATP-consuming power stroke potentials try to center-position the nucleosome with respect to the DNA strand. Finally, the active translocation time in the dynamical FRET time traces reveals that the diffusion constant of the nucleosome-remodeler complex, D_{NR}, depends on ATP concentration, by applying the Einstein force scale. A simple reasoning shows that lowering the histone-DNA adsorption energy elevates the thermal diffusion constant D_{NR} by a factor up to 10–100, possibly due to a highly loosened DNA state during active repositioning.

We reconsidered the issue of proper sampling between the two SNF2h motors in hACF. An analysis was presented of when the desynchronization between the two SNF2h becomes appreciable. A sampling rate reduced by a factor of 10 produces nucleosomal states with equal probability among the ℓ states, or among discrete intermediates in the previous two-motor model. This theoretical outcome is experimentally observed in the case of SNF2h alone, while hACF generates mainly center-positioned nucleosomes [12]. Since SNF2h acts cooperatively, we may speculate that the noncatalytic subunit of Acf1 in hACF is required for a proper synchronization between the two SNF2h motors.

ACKNOWLEDGMENT

Y.V. thanks the Région Nord-Pas de Calais for support by a postdoctoral grant via the CPER.

APPENDIX: CONFINEMENT POTENTIAL

With the extension of the interval [0,80] to [−40,120] for the possible ℓ states, a confinement potential is introduced to compensate for the liberated histone-DNA contacts ($6k_BT$ per histone-DNA contact). The analytic expression we employ is

$$U_c(\ell) = A(e^{-\ell/\delta} + e^{(\ell-80)/\delta}). \tag{A1}$$

Here, we choose $A = 0.5k_BT$ and $\delta = 10$ bp to reach $\approx 24k_BT$ at $\ell = -40$ bp (four histone-DNA contacts are broken). However, the main issue is to inhibit probability flux at the boundaries. The shape of the confinement potential, or the exact values, are of less importance in the extended regions. In the [0,80] range, the potential is negligible, as it should be.

[1] G. D. Bowman, Curr. Opin. Struct. Biol. **20**, 73 (2010).
[2] R. Blossey and H. Schiessel, FEBS J. **278**, 3619 (2011).
[3] L. R. Racki *et al*., Nature (London) **462**, 1016 (2009).
[4] G. J. Narlikar, Curr. Opin. Chem. Biol. **14**, 660 (2010).
[5] Y. Vandecan and R. Blossey, Phys. Rev. E **85**, 061920 (2012).
[6] H. Wang and G. Oster, Appl. Phys. A: Mater. Sci. Process. **75**, 315 (2002).
[7] P. Gaspard and E. Gerritsma, J. Theor. Biol. **247**, 672 (2009).
[8] B. R. Cairns, Nat. Struct. Mol. Biol **14**, 989 (2007).
[9] G. Sirinakis, C. R. Clapier, Y. Gao, R. Viswanathan, B. R. Cairns, and Y. Zhang, EMBO J. **30**, 2364 (2011).
[10] V. K. Gangaraju, P. Prasad, A. Srour, M. N. Kagalwala, and B. Bartholomew, Mol. Cell **35**, 58 (2009).
[11] M. E. Fisher and A. B. Kolomeisky, Proc. Natl. Acad. Sci. USA **96**, 6597 (1999).
[12] J. G. Yang, T. S. Madrid, E. Sevastopoulos, and G. J. Narlikar, Nat. Struct. Mol. Biol. **13**, 1078 (2006).
[13] H. Schiessel, J. Phys.: Condens. Matter **15**, R699 (2003).
[14] T. R. Blosser, J. G. Yang, M. D. Stone, G. J. Narlikar, and X. Zhuang, Nature (London) **462**, 1022 (2009).
[15] G. Lia, M. Inderri, T. Owen-Hughes, L. Finzi, A. Podesta, P. Milani, and D. Dunlap, J. Biophotonics **1**, 280 (2008).
[16] L. R. Racki and G. J. Narlikar, Curr. Opin. Gen. Dev. **18**, 137 (2008).
[17] R. Lipowsky and N. Jaster, J. Stat. Phys. **110**, 1141 (2003).
[18] T. Ito, M. E. Levenstein, D. V. Fyodorov, A. K. Kutach, R. Kobayashi, and J. T. Kadonaga, Gen. Dev. **13**, 1529 (1999).
[19] X. He, H. Y. Fan, G. J. Narlikar, and R. E. Kingston, J. Biol. Chem. **281**, 28636 (2006).
[20] A. Flaus and T. J. Richmond, J. Mol. Biol. **275**, 427 (1998).
[21] H. Schiessel, J. Widom, R. F. Bruinsma, and W. M. Gelbart, Phys. Rev. Lett. **86**, 4414 (2001).
[22] I. M. Kulic and H. Schiessel, Biophys. J. **84**, 3197 (2003).